

# Stiction failure in microswitches due to elasto-plastic adhesive contact

Ling Wu<sup>1,2</sup>, Jean-Claude Golinval<sup>1</sup>, Ludovic Noels<sup>1</sup>

<sup>1</sup>University of Liege, Aerospace and Mechanical Engineering Department  
Chemin des Chevreuils 1, B4000 Liège, Belgium  
{L.Wu,JC.Golinval,L.Noels}@ulg.ac.be

<sup>2</sup>Northwestern Polytechnical University, School of Aeronautics  
710072 Xi'an, China

## ABSTRACT

Undesirable stiction, which results from contact between surfaces, is a major failure mode in micro-switches. Indeed the adhesive forces can become so important that the two surfaces remain permanently glued, limiting the life-time of the MEMS. This is especially true when contact happens between surfaces where elasto-plastic asperities deform permanently until the surfaces reach plastic accommodation, increasing the surface forces. To predict this behavior, a micro adhesive-contact model is developed, which accounts for the surfaces topography evolutions during elasto-plastic contacts. This model can be used at a higher scale to study the MEMS behavior, and thus its life-time. The MEMS devices studied here are assumed to work in a dry environment. In these operating conditions only the Van der Waals forces have to be considered for adhesion. For illustration purpose, an electrostatic-structural analysis is performed on a micro-switch. To determine the degree of plasticity involved, the impact energy of the movable electrode at pull-in is estimated. Thus the maximal adhesive force is predicted using the developed model.

## 1. INTRODUCTION

The inherent characters of MEMS such as the large surface area-to-volume ratio, smooth surfaces, small interfacial gaps and small restoring forces, make them particularly vulnerable to stiction which is one of the most common failure mechanism of MEMS [1]. Stiction happens when two components entering into contact permanently adhere to each-other because the restoring forces are smaller than the surface forces (capillary, van der Waals (VDW) or electrostatic). This can happen either during the fabrication process at etching (release stiction) or during normal use (in-use stiction).

To improve the reliability of MEMS, models are required in order to predict and avoid in-use stiction failure. A multi-scale model can predict at the lower scale the adhesive contact forces of two rough surfaces, and thus can integrate these curves on the surface of the finite elements as a contact law at the higher scale [2, 3]. The authors recently proposed [4] a model predicting the micro adhesive-contact curves, i.e. the adhesive-contact force vs. surface separation distance, for two interacting micro-surfaces. This analytical model, accounting for elastic deformation of the asperities, and for van der Waals forces, is based on classical adhesion theories [5-10] and can be easily integrated in the multiscale framework [2, 3].

Although the two-scale framework [3] based on the elastic micro-model [4] has been shown to predict accurate results for elastic material in dry environment [3], in order to extend the applicability of the method to other environments, the micro-model requires enhancements, and in particular its extension to the elasto-plastic behavior of the asperities. As a first step toward this end, this paper presents an improved model for the single elastic-plastic asperity-plane interaction problem.

When elastic-plastic rough surfaces interact, each asperity will be affected differently due to the statistical nature of the asperity distribution on the surfaces: higher asperities will experience plastic deformations first. Due to the plastic behavior, the contact force on deformed asperities is lower than in the elastic case for the same contact interference (distance between undeformed profiles), while adhesive force increases due to the change of asperity profile. Because of the combination of these two phenomena the pull-out force - maximum attractive forces or the minimum compressive forces between the two interacting surfaces - is higher than that between two pure elastic contacting rough surfaces. Another qualitative difference with elastic surfaces is the difference of behavior under cyclic loading: after repeating contacts, the distribution of asperities height and the tip radii of the higher asperities change [11], until plastic accommodation or shakedown [12]. This induces a “contact hardening” [13] and the pull-out force increases until accommodation, unless in-use stiction happens first.

To account for elasto-plastic behavior, the authors [14] have developed a micro-model able to predict stiction for elastic-plastic rough surfaces by first considering the problem of a single elasto-plastic asperity interaction and thus the generalization to the interaction of rough surfaces. The single asperity/plane contact problem is modeled using semi-analytical models [15-17] which allow evaluating the deformed asperity profile during hysteretic loading/unloading without considering the adhesion effect. Assuming adhesion will not affect the plastic deformations, which is not the case for extremely soft materials as gold [18], we can consider the Maugis theory [7] completed by Kim expansion [8] to evaluate the adhesion forces during the unloading phase [4] from the tip radius evolution during loading process. As a main difference with previous models [15-17], adhesion forces are evaluated taking into account the effect of the non-constant asperity curvature resulting from elasto-plastic deformations, which conducts to an accurate prediction of the pull-out forces [14]. In this model only van der Waals forces are considered, which is a realistic assumption below 30% humidity [1]. The interaction of two rough surfaces is achieved by considering a usual statistical distribution of asperities [5-6], however, contrarily to the elastic case, the distribution of asperities heights and the asperity profiles of the higher asperities change due to the plastic deformations. These changes, and the resulting adhesive-contact forces, are evaluated using the single asperity model. As a result, micro adhesive-contact curves of two interacting elasto-plastic rough surfaces can be predicted in an analytical way for loading and unloading.

The purpose of this paper is to predict the reliability of a micro-switch by considering the effect of repeated interactions between the movable/substrate electrodes. For illustration purpose a one-dimensional model is considered and contact occurs between two Ruthenium (Ru) films. We also show that unloading curves change after repeated interactions until reaching accommodation. Thus, the pull-out force can be predicted in terms of the pull-in force and of the cycle number, opening the way to stiction-free design.

Organization of the paper is as follows. In section 2, the micro-model for elasto-plastic adhesive-contact is summarized. First the single elasto-plastic asperity/plane interaction model with no adhesion effect is described. Then, the adhesion forces are evaluated from the deformed asperity profile taking into account the effect of the non-constant asperity curvature resulting from elasto-plastic deformations. Finally the micro adhesive-contact curves of two interacting elasto-plastic rough surfaces

are deduced. This model can then be used in section 3 to study the micro-switch reliability. In particular the effect of cyclic loading on the pull-out force, and thus on the stiction risk, is predicted.

## 2. MICRO-MODEL FOR ELASTO-PLASTIC ADHESIVE-CONTACT

In this section, the single elasto-plastic asperity/plane interaction model with no adhesion effect is first described before evaluating the adhesion forces from the deformed asperity profile. Then, using a statistical distribution of asperities heights accounting for the changes in asperity profiles and height due to the plastic deformations, the micro adhesive-contact curves of two interacting elasto-plastic rough surfaces can be predicted.

### 2.1. Single Asperity Elasto-Plastic Contact

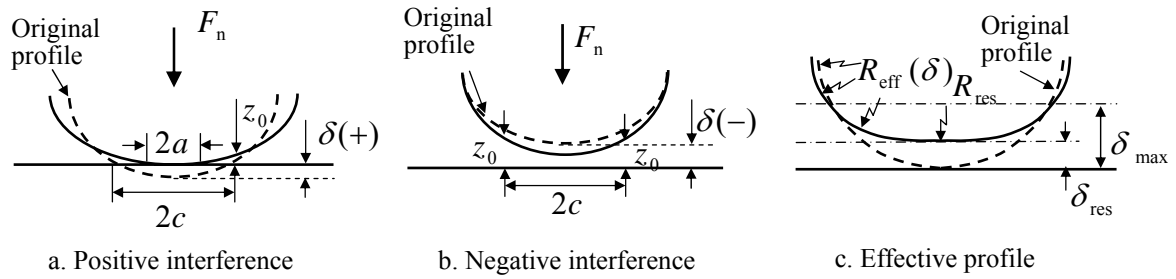


Fig. 1 Definition of single asperity interference [14]

Let an asperity of tip radius  $R$ , Young modulus  $E$ , and yield stress  $S_Y$ , interacts with a rigid plane at an interference distance  $\delta$ , positive in case of contact and negative otherwise, see Fig. 1a and Fig. 1b, defined as the distance between the original profile of the asperity tip and the plane. When the plane starts interacting with the asperity during loading, the critical yield interference  $\delta_{CP}$  is defined as the interference at which the asperity starts yielding and can be expressed as [15-17]

$$\frac{\delta_{CP}}{R} = \left( \frac{\pi C_v S_Y}{2E} \right)^2 \quad (1)$$

In this expression  $C_v$  is a coefficient that depends on the Poisson ratio  $\nu$ , and that can be evaluated from  $C_v = 1.295e^{0.736\nu}$ , e.g. [16]. As, with our assumption, the asperity starts yielding at positive interference, there exists a corresponding critical contact radius  $a_{CP}$ , Fig. 1a, and a critical contact force  $F_{CP}$  respectively evaluated as

$$a_{CP} = \sqrt{\frac{\delta_{CP}}{R}} \quad (2)$$

$$\frac{F_{CP}}{R} = \frac{2}{3} \pi C_v S_Y \delta_{CP} \quad (3)$$

During the loading phase, assuming the interference goes beyond the critical interference  $\delta_{CP}$ , the asperity is subject to permanent plastic deformations that depend on  $\delta_{max}$  the maximal interference reached. After unloading, the asperity exhibits a permanent reduction of the asperity height  $\delta_{res}$ , and a modified asperity tip radius  $R_{res}$ , see Fig. 1c, that were curved fitted from finite element numerical simulations [17]

$$\frac{\delta_{\text{res}}}{\delta_{\text{rmax}}} = \left[ 1 - \left( \frac{\delta_{\text{CP}}}{\delta_{\text{rmax}}} \right)^{0.28} \right] \left[ 1 - \left( \frac{\delta_{\text{CP}}}{\delta_{\text{rmax}}} \right)^{0.69} \right] \quad (4)$$

$$\frac{R_{\text{res}}}{R} = 1 + 1.275 \left( \frac{S_Y}{E} \right)^{0.216} \left( \frac{\delta_{\text{max}}}{\delta_{\text{CP}}} - 1 \right) \quad (5)$$

## 2.2. Single Asperity Elasto-Plastic adhesive contact

In Maugis theory [7], the inter-atomic attraction effect is modeled using a Dugdale assumption: within a critical value of separation  $z_0$ , two surfaces are attracted with a constant force per unit area  $\sigma_0$ , while if the separation  $z$  exceeds  $z_0$ , the adhesive traction vanishes. The associated adhesive energy reads  $\varpi = \sigma_0 z_0$ . Maugis theory for the interaction of two elastic asperities characterized by two Young modulus  $E_1$  and  $E_2$ , two Poisson ratio  $\nu_1$  and  $\nu_2$ , and by two tip radii  $R_1$  and  $R_2$ , is based on the definition of a transition parameter

$$\lambda = \frac{2\sigma_0}{\sqrt[3]{\frac{\pi\varpi K^2}{R}}} \quad \text{where} \quad K = \frac{4}{3} \left( \frac{1-\nu_1^2}{E_1} + \frac{1-\nu_2^2}{E_2} \right)^{-1} \quad \text{and} \quad R = \frac{R_1 R_2}{R_1 + R_2} \quad (6)$$

are respectively the equivalent modulus and initial tip radius of two interacting asperities, or the initial radius of an asperity interacting with a plane. The transition parameter allows defining a solution ranging from JKR regime [5] - soft materials with a large contact curvature surface and with a high surface energy – to the DMT regime [6] - hard materials with a reduced contact curvature and with a low surface energy. This solution provides, for a given interaction  $\delta$ , the adhesive contact force  $F_n$ , the interacting contact radius  $a$  and the adhesive-contact radius  $c$  on which adhesive forces apply, see Fig. 1a. The system of equations is written in terms of the non-dimensional values

$$A = a \left( \frac{K}{\pi\varpi R^2} \right)^{1/3}, \quad \bar{F}_n = \frac{F_n}{\pi\varpi R}, \quad \Delta = \delta \left( \frac{K^2}{\pi^2\varpi^2 R} \right)^{1/3} \quad \text{and} \quad m = \frac{c}{a} \quad (7)$$

and reads

$$1 = \frac{\lambda A^2}{2} \left[ \sqrt{m^2 - 1} + (m^2 - 2) \arctan \sqrt{m^2 - 1} \right] + \frac{4\lambda^2 A}{3} \left[ \sqrt{m^2 - 1} \arctan \sqrt{m^2 - 1} - m + 1 \right] \quad (8)$$

$$\Delta = A^2 - \frac{4\lambda A}{3} \sqrt{m^2 - 1} \quad (9)$$

$$\bar{F}_n = A^3 - \lambda A^2 \left[ \sqrt{m^2 - 1} + m^2 \arctan \sqrt{m^2 - 1} \right] \quad (10)$$

This set of equations is completed by the interference evaluation

$$\delta = \frac{a^2}{R} - \frac{8\sigma_0}{3K} \sqrt{c^2 - a^2} \quad (11)$$

Kim et al. [8] extended Maugis-Dugdale solution to the non-contact regime when  $a = 0$  and  $c \neq 0$ , see Fig. 1b, see [4] for details. Practically, this expansion has to be considered when  $\lambda < 0.938$ .

Although this adhesive theory is based on Hertz contact model, and thus assumes elastic behavior, we proposed [14] to apply this theory on the permanently deformed asperity profile. As during the unloading the behavior remains elastic, at the

exception of extremely soft materials, Maugis theory completed by Kim extension constitutes a good approximation. However, we proposed to account for a non-constant asperity radius in terms of the interference, see Fig. 1c, and to perform the adhesive-contact theory on the assumed elastically deformed asperity, which has an effective tip radius  $R_{\text{eff}}$  at a contact interference  $\delta - \delta_{\text{res}}$ . This is motivated by the fact that Maugis theory assumes a uniform asperity radius to apply Hertz theory although this case is only met at the limit case  $\delta = \delta_{\text{res}}$ . The following expression has been proposed [14]

$$\frac{R_{\text{eff}}}{R} = \frac{R_{\text{res}}}{R} - 1.275(1 - c_1) \left( \frac{S_Y}{E} \right)^{0.216} \left( \frac{\delta_{\text{max}}}{\delta_{\text{CP}}} - 1 \right) \left( \frac{1 - e^{-c_2 \frac{\delta - \delta_{\text{res}}}{\delta_{\text{max}} - \delta_{\text{res}}}}}{1 - e^{-c_2}} \right) \quad (12)$$

In this expression,  $c_1$  and  $c_2$  are functions that have to be determined by inverse analysis from finite-element results. Using the simulations performed for Ru [19], we proposed [14]

$$c_1 = 0.22 + 0.6242e^{-0.092 \frac{\delta_{\text{max}}}{\delta_{\text{CP}}}} \quad \text{and} \quad c_2 = \frac{10}{1 + (\delta_{\text{max}}/10\delta_{\text{CP}})^2} - 5 \quad (13)$$

Because of the elasto-plastic behavior happening during contact, the theory developed here results in different adhesive-contact forces during loading  $F_n^L(\delta)$  and unloading  $F_n^U(\delta)$ . During loading phase, once  $\delta_{\text{CP}}$  is reached, the maximum interference is identical to the current one ( $\delta_{\text{max}} = \delta$ ) and the deformed profile can be evaluated from (4)-(5). Thus, the loading force  $F_n^L(\delta)$  is evaluated from Maugis solution by solving the system (8)-(11), with as input for  $R$  the effective radius (12), and as input for  $\delta$  the effective value  $\delta - \delta_{\text{res}}$ , where  $\delta_{\text{res}}$  increasing during the whole loading process. During unloading however, the residual ( $\delta_{\text{res}}$ ) and maximal ( $\delta_{\text{max}}$ ) interferences reached remain constant. The adhesive-contact force during unloading  $F_n^U(\delta)$  is computed from the Kim extension [8] of Maugis theory [7], with as input for  $R$  the effective radius (12), and as input for  $\delta$  the effective value  $\delta - \delta_{\text{res}}$ . Contrarily to the loading process, the effect of adhesion needs to be considered at the intermediate pull-out stage, which is achieved by using the Kim extension [8].

Table 1 Properties of Ru films

$R$ [ $\mu\text{m}$ ]	4
$E$ [GPa]	410
$\nu$ [-]	0.3
$S_Y$ [GPa]	3.42
$z_0$ [nm]	0.169
$\varpi$ [ $\text{J}/\text{m}^2$ ]	1
$\sigma_s$ [nm]	7.78
$R_q$ [nm]	7.81
$N$ [ $\mu\text{m}^2$ ]	10

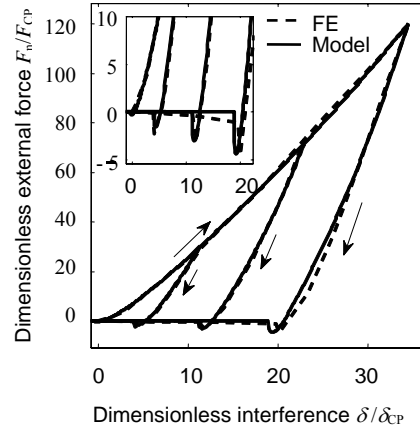


Fig. 2 Comparison of the single asperity model with finite element

The elastic-plastic adhesive contact of a micro sphere was studied for Ruthenium (Ru) in [19]. Ru has the advantage of not exhibiting plastic deformation under adhesive effects only. Material properties and initial asperity tip radius are reported in Table 1. To demonstrate the accuracy of the proposed method, Fig. 2 compares the predicted adhesive-contact forces to the FE results for the loading and unloading adhesive-contact forces at three maximum interferences  $\delta_{\text{max}}$  successively equal to 17, 34 and 51 nm. It is seen that an excellent agreement is obtained for the three loading conditions.

### 2.3. Rough Surfaces Interaction

Greenwood and Williamson ‘asperity-based model’ [9] is applied to simulate the rough surface/plane interaction. A rough surface is described by a collection of spherical asperities with identical end radii  $R$ , whose height  $h$  have a statistical distribution

$$\varphi(h) = \frac{1}{\sigma_s \sqrt{2\pi}} \exp\left(\frac{-h^2}{2\sigma_s^2}\right) \quad (14)$$

where  $\sigma_s$  is the standard deviations in asperity heights. The contact of two rough surfaces can be represented by the contact between an equivalent rough surface and a smooth plane [10]: if the two initial contacting rough surfaces have respectively the asperities end radii of  $R_1$  and  $R_2$ , the equivalent radius is defined by (6), and if the standard deviation in asperity heights are  $\sigma_{s1}$  and  $\sigma_{s2}$ , the equivalent rough surface is defined by the standard deviation in asperity heights  $\sigma_s = (\sigma_{s1}^2 + \sigma_{s2}^2)^{1/2}$ . The interaction between two rough surfaces is also characterized by the distance  $d$  between the two rough surface mean planes of asperity heights, and by  $N$  the surface density of asperities. All these values can be identified from the study of the surfaces topography, and, in particular, depend on the surface RMS roughness  $R_q$ , see [3] for details.

The surface loading and unloading forces, respectively  $F_{n\Gamma}^L$  and  $F_{n\Gamma}^U$  can now be evaluated by integrating on the surface the effect of each asperity, for which the interference reads  $\delta = h - d$ , using the framework described in section 2.2. Toward this end, non-dimensional values are defined

$$\bar{F}_{n\Gamma} = \frac{F_{n\Gamma}}{\pi \omega R} \quad , \quad \bar{d} = d^3 \sqrt{\frac{K^2}{\pi^2 \omega^2 R}} \quad \text{and} \quad \bar{\sigma}_s = \sigma_s^3 \sqrt{\frac{K^2}{\pi^2 \omega^2 R}} \quad (15)$$

which allows writing

$$\bar{F}_{n\Gamma} = \frac{N}{\bar{\sigma}_s \sqrt{2\pi}} \int \bar{F}_n(\Delta) e^{-\frac{(\Delta+d)^2}{2\bar{\sigma}_s^2}} d\Delta \quad (16)$$

It bears emphasize that as asperities enter into plasticity for different surface distances, the effective profile is different for each asperity. Details on the integration (16) are provided in [14].

### 3. CYCLIC LOADING OF A MICRO-SWITCH

Table 2 Properties of the micro-switch

$d_0$ [ $\mu\text{m}$ ]	2
$t_d$ [ $\mu\text{m}$ ]	0.15
$\varepsilon_0$ [pF/m]	8.854
$\varepsilon_d / \varepsilon_0$ [-]	7.6
$t_s$ [nm]	180

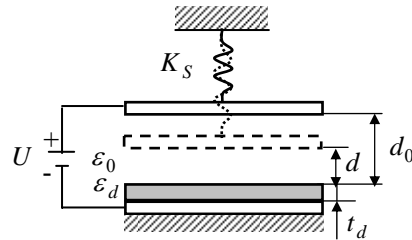


Fig. 3 1D micro-switch application

A one-dimensional model of micro-switch is considered, see Fig. 3. In this model, a potential difference  $U$  is applied between a movable electrode and a substrate electrode covered by a dielectric layer of thickness  $t_d$  and permittivity  $\varepsilon_d$ . The movable electrode is attached to a spring of stiffness per unit area  $K_s$ , and is initially at a distance  $d_0$  from the substrate. The switch is supposed to work in vacuum, permittivity  $\varepsilon_0$ , so the damping effect of squeeze film is neglected. Typical values for SiN

dielectric are reported in Table 2. Contact is assumed to occur between two Ru surfaces, for which typical topography values are reported in Table 1. Ru films of thickness  $t_s$  are deposited on the movable electrode, and also on a part of the substrate.

From these data, the pull-in voltage and the impact energy can be computed in terms of the stiffness  $K_S$ . This computation has been performed in [14], and in this application we consider an impact energy of  $E_I=0.5 \text{ J/m}^2$ . This impact energy per unit surface of the contacting area affects the plastic deformation of the asperities and thus the adhesion-contact forces. Indeed, once impact occurs, the energy  $E_I$  is converted into elastic and plastic deformations energies. The asperities loading process finishes once all the energy has been converted. The energy for elastic wave propagation is neglected in this work; however elastic energy in the Ru film is accounted for. With these assumptions, the distance  $d_e$  between the two rough surfaces mean planes of asperity heights reached at the end of the impact process is deduced from

$$E_I = \int_{d_e}^{\infty} F_{nT}^L(d) dd + \frac{[F_{nT}^L(d_e)]^2 t_s}{2E} \quad (17)$$

Once the distance  $d_e$  has been computed, the deformed profile of the asperities is known, and the unloading process can be studied. In particular, the adhesive contact forces  $F_{nT}^U$  are evaluated from (16) in terms of the distance  $d > d_e$ .

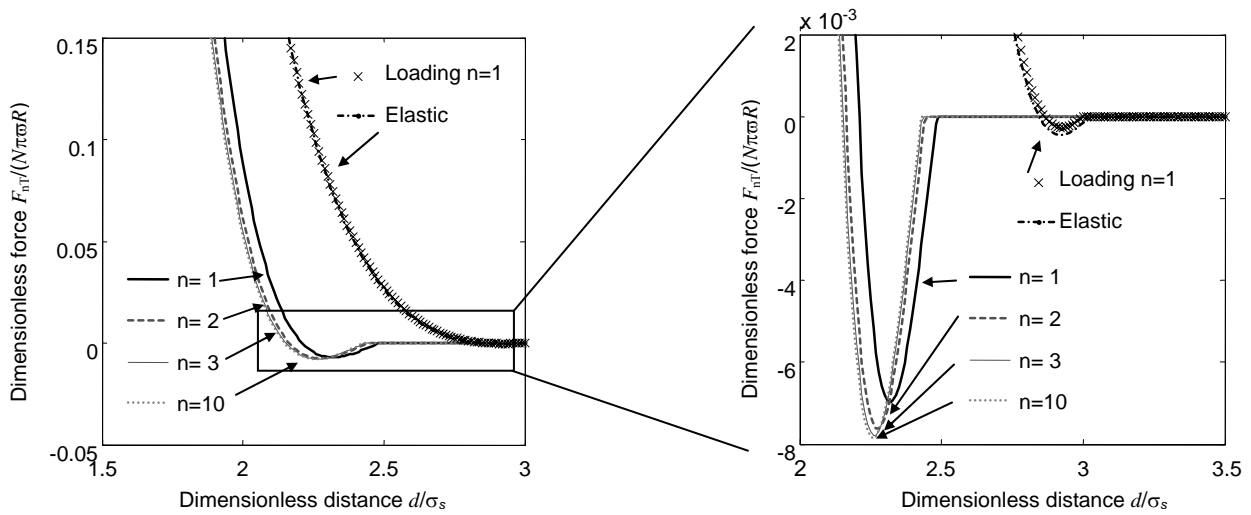


Fig. 4 Cyclic loading of the 1D micro-switch

These two steps characterize one loading/unloading cycle. To study cyclic loading, the same analyses have to be performed with updated asperities profiles. Indeed, after the first cycle, the profile of the surface is modified as only higher asperities entered into contact and exhibited plastic deformations. History is tracked by keeping after each loading the function  $\delta_{\max}(h)$  of the maximal interference reached for an asperity of initial height  $h$ . From this function the profile change of an asperity of initial height  $h$  can be known to evaluate its effect on the loading/unloading forces (16). Thus, the reliability of the micro-switch can be studied by considering the effect of repeated interactions between the movable/substrate electrodes. Indeed, the unloading curves change after repeated interactions until reaching accommodation, as illustrated on Fig. 4, where the unloading curves after 1, 2, 3 and 10 cycles are reported. From this figure it appears that the pull-out force after accommodation can be predicted, opening the way to stiction-free design. On this figure the elastic solution is also reported, and is shown to underestimate the pull-out force. Also the loading curve is represented.

## 4. CONCLUSIONS

In order to predict stiction in MEMS structures, a possible approach is to consider a multi-scale framework. If at the higher scale a finite element analysis can be considered, it requires an adhesive-contact law to be integrated on the interacting surfaces.

The definition of this adhesive-contact law constitutes the micro-scale problem. In this paper, this adhesive contact-distance curve of two interacting elasto-plastic rough surfaces was established using a semi-analytical analysis. First the deformed profile of the asperity is evaluated from literature models, which uncouple the plastic deformation from the adhesive effect. This assumption usually holds except for materials suffering from jump-in induced plasticity, as for gold, for which the sole adhesion effect can lead to plastic deformations. Then, we use Maugis-Kim adhesive theory to evaluate the adhesive-contact forces. In order to account for the deformed shape of the asperity, assumed as spherical in Hertz contact of Maugis theory, we propose to evaluate an effective asperity radius which depends on the interference. With this method, we can predict the loading/unloading hysteresis curves of a single elastic-plastic asperity interacting with a rigid plane. Finally a statistical model of asperity height is considered to study the interaction of two elasto-plastic rough surfaces.

The predictions of this model are illustrated by considering the cyclic loading of a 1D micro-switch application. It is shown that the repeated loading of a MEMS switch changes the structure of the contacting surface due to the plastic deformations. Thus, with time, the contact surfaces become smoother, increasing the adhesion effect. This effect should be considered at design stage to avoid in-use stiction.

## REFERENCES

- [1] Van Spengen W., Puers R., and DeWolf I. On the physics of stiction and its impact on the reliability of microstructures. *Journal of Adhesion Science and Technology*, 17(4):563–582, 2003.
- [2] Do C., Hill M., Lishchynska M., Cychowski M., and Delaney K. Modeling, simulation and validation of the dynamic performance of a single-pole single-throw RF-MEMS contact switch. In *Thermal, Mechanical & Multi-Physics Simulation, and Experiments in Microelectronics and Microsystems (EuroSimE)*, 2011 12th International Conference on, pages 1–6, April 2011. Linz, Austria.
- [3] Wu L., Noels L., Rochus V., Pustan M., and Golinval J.-C. A micro-macroapproach to predict stiction due to surface contact in microelectromechanical systems. *Journal of Microelectromechanical Systems*, 20(4):976–990, 2011.
- [4] Wu L., Rochus V., Noels L., and Golinval J.-C. Influence of adhesive rough surface contact on microswitches. *Journal of Applied Physics*, 106(11):113502–1 – 113502–10, 2009.
- [5] Johnson K., Kendall K., and Roberts A. Surface energy and the contact of elastic solids. *Proceedings of the Royal Society of London A*, 324(1558):301–313, 1971.
- [6] Derjaguin B., Muller V., and Toporov Y. Effect of contact deformation on the adhesion of elastic solids. *Journal of Colloid and Interface Science*, 53(2):314–326, 1975.
- [7] Maugis D. Adhesion of spheres: The JKR/DMT transition using a dugdale model. *Journal of Colloid and Interface Science*, 150(1):243–269, 1992.
- [8] Kim K., McMeeking R., and Johnson K.. Adhesion, slip, cohesive zones and energy fluxes for elastic spheres in contact. *Journal of the Mechanics and Physics of Solids*, 46(2):243–266, 1998.
- [9] Greenwood J. and Williamson J. Contact of nominally flat surfaces. *Proceedings of the Royal Society of London A*,



295(1442):300–319, 1966.

- [10] Greenwood J. and J. Tripp J. The contact of two nominally flat rough surfaces. *Proceedings of the Institution of Mechanical Engineers 1847-1996*, 185(1970):625–633, 1971.
- [11] Jones R. Models for contact loading and unloading of a rough surface. *International Journal of Engineering Science*, 42(17-18): 1931 –1947, 2004.
- [12] Williams, J. The influence of repeated loading, residual stresses and shakedown on the behaviour of tribological contacts. *Tribology International*, 38(9): 786 – 797, 2005.
- [13] Majumder S., McGruer N., Adams G., Zavracky P., Morrison R., and Krim J. Study of contacts in an electrostatically actuated microswitch. *Sensors and Actuators A: Physical*, 93(1):19 – 26, 2001.
- [14] Wu L., Golinval J.-C. and Noels L. A micro model for elasto-plastic adhesive-contact in micro-switches. *ASME Journal of Applied Mechanics*, Submitted.
- [15] Chang W., Etsion I., and Bogy D. An elasticplastic model for the contact of rough surfaces. *Journal of Tribology*, 109(2):257–263, 1987.
- [16] Jackson R., and Green I. A finite element study of elasto-plastic hemispherical contact against a rigid flat. *Journal of Tribology*, 127(2): 343– 354, 2005.
- [17] Etsion I., Kligerman Y., and Kadin Y. Unloading of an elastic-plastic loaded spherical contact. *International Journal of Solids and Structures*, 42(13):3716 – 3729, 2005.
- [18] Kadin Y., Kligerman Y., and Etsion I. Cyclic loading of an elasticplastic adhesive spherical microcontact. *Journal of Applied Physics*, 104(7): 073522–1–073522–8, 2007.
- [19] Du Y., Chen L., McGruer N., Adams G. and Etsion I. A finite element model of loading and unloading of an asperity contact with adhesion and plasticity. *Journal of Colloid and Interface Science*, 312(2):522 – 528, 2007.